

**Neptune and Company Inc.**

June 1, 2011 Report for EnergySolutions

Clive DU PA Model, version 1

**Appendix 3**

Embankment Modeling

# Embankment Modeling for the Clive DU PA Model

28 May 2011

Prepared by  
Neptune and Company, Inc.

This page is intentionally blank, aside from this statement.

## CONTENTS

FIGURES .....	iv
TABLES.....	v
1.0 Summary of Parameter Values.....	1
2.0 Introduction .....	2
3.0 Physical Dimensions .....	2
3.1 Class A South Embankment Dimensions .....	3
3.1.1 Class A South Embankment Interior Waste.....	4
3.1.2 Class A South Cover and Liner Dimensions.....	6
4.0 Original Grade Elevation .....	10
4.1 Class A South Embankment Original Grade .....	10
5.0 Implementation in the GoldSim Model.....	11
5.1 Representation of the CAS Embankment .....	11
5.1.1 CAS Embankment Dimensions.....	12
5.1.2 CAS Columns.....	12
6.0 References .....	14

## FIGURES

Figure 1. The Clive Facility, with the location of the Class A South embankment outlined in green. This orthophotograph is roughly 1 mile across, and north is up. ....	3
Figure 2. Section and Plan views of the Class A South embankment, with top slope shown in blue and side slope in green. The brown dotted line in the West-East Cross section represents below-grade (below the line) and above-grade (above the line) regions of the embankment. ....	4
Figure 3. Dimensions of the Class A South embankment that are used in the Clive DU PA model. ....	5
Figure 4. Class A South and 11e.(2) cell engineering drawing 07021 V1. ....	7
Figure 5. Class A South and 11e.(2) cell engineering drawing 07021 V3. ....	8
Figure 6. Class A South cell engineering drawing 07021 V7: cap dimensions. ....	9
Figure 7. Section 32 within the Aragonite quadrangle, as it appeared in 1973, before construction of the Clive Facility. Note elevation contours at 4270 and 4280 ft amsl. <i>ARAGONITE NW</i> is the next quadrangle to the west. ....	11
Figure 8. Geometrical deconstruction of the CAS cell waste volumes. ....	12
Figure 9. Waste layering definitions within the two columns of the CAS cell. ....	13

## **TABLES**

Table 1. Summary of embankment engineering parameters ..... 1  
Table 2. Cover layer thicknesses for the CAS cell..... 10

## 1.0 Summary of Parameter Values

The parameters that define the characteristics of the Class A South embankment at the Clive facility are summarized in Table 1. Following this summary are sections describing the basis for these values. Of principal interest to the model are the interior dimensions of the volume occupied by waste, and the thicknesses of the various layers in the engineered cover.

**Table 1. Summary of embankment engineering parameters**

parameter	value	units	reference / comment
average original grade elevation	4272	ft amsl*	USGS (1973) see §4.1 below
elevation of top of the waste at the ridgeline	4317.25	ft amsl	EnergySolutions (2009) see eq. (1) in §3.1.1
elevation of top of the waste at the break in slope	4299.20	ft amsl	EnergySolutions (2009) see eq. (2) in §3.1.1
average elevation of the bottom of the waste	4264.17	ft amsl	EnergySolutions (2009) see eq. (3) in §3.1.1
average elevation of the bottom of the clay liner	4262.17	ft amsl	see eq. (6)(3) in §3.1.2
length overall	1429.6	ft	EnergySolutions (2009) see eq. (4) in §3.1.1
width overall	1775.0	ft	EnergySolutions (2009) see eq. (5) in §3.1.1
length from edge to the break in slope	153.2	ft	EnergySolutions (2009) see §3.1.1
width from edge to the break in slope	152.1	ft	<i>ibid.</i>
length along the ridge	542.1	ft	<i>ibid.</i>
type A rip rap thickness	18	in	EnergySolutions (2009) see Table 2
type B rip rap thickness	18	in	<i>ibid.</i>
type A filter zone thickness	6	in	<i>ibid.</i>
sacrificial soil thickness	12	in	<i>ibid.</i>
type B filter zone thickness (top slope only)	6	in	<i>ibid.</i>
type B filter zone thickness (side slope only)	18	in	<i>ibid.</i>
$5 \times 10^{-8}$ cm/s radon barrier clay thickness	12	in	<i>ibid.</i>
$1 \times 10^{-6}$ cm/s radon barrier clay thickness	12	in	<i>ibid.</i>
clay liner thickness	24	in	Whetstone (2000) see end of §3.1.2

\* above mean sea level

## 2.0 Introduction

The safe storage and disposal of depleted uranium (DU) waste is essential for mitigating releases of radioactive materials and reducing exposures to humans and the environment. Currently, a radioactive waste facility located in Clive, Utah (the “Clive facility”) operated by the company EnergySolutions Inc. is being considered to receive and store DU waste that has been declared surplus from radiological facilities across the nation. The Clive facility has been tasked with disposing of the DU waste in a manner that protects humans and the environment from future radiological releases.

To assess whether the proposed Clive facility location and containment technologies are suitable for protection of human health, specific performance objectives for land disposal of radioactive waste set forth in Utah Administrative Code (UAC) Rule R313-25 *License Requirements for Land Disposal of Radioactive Waste - General Provisions* must be met—specifically R313-25-8 *Technical Analyses*. In order to support the required radiological performance assessment (PA), a probabilistic computer model has been developed to evaluate the doses to human receptors and concentrations in groundwater that would result from the disposal of radioactive waste, and conversely to determine how much waste can be safely disposed at the Clive facility. The GoldSim systems analysis software (GTG, 2010) was used to construct the probabilistic PA model.

The site conditions, chemical and radiological characteristics of the wastes, contaminant transport pathways, and potential human receptors and exposure routes at the Clive facility that are used to structure the quantitative PA model are described in the conceptual site model documented in the white paper entitled *Conceptual Site Model for Disposal of Depleted Uranium at the Clive Facility* (Clive DU PA CSM.pdf).

The purpose of this white paper is to address specific details relating to the dimensional components of the Class A South (CAS) section of the Federal Cell, located at the Clive facility. This paper is organized to give a brief overview of where the CAS section is located at the Clive facility followed by a description of the parameters and calculations used to estimate the various dimensional components of the CAS embankment.

This probabilistic PA takes into account uncertainty in many input parameters, but the dimensions of the CAS embankment are not considered to be uncertain. Given that the disposal cell is carefully designed and constructed, any uncertainty in its dimensions is considered insignificant. Stochastic representation of parameters is reserved for those values about which there is uncertainty.

## 3.0 Physical Dimensions

The Clive DU PA model considers only a single embankment. For the purposes of this PA, only the CAS section of the Federal Cell is considered for disposal (Figure 1).

### 3.1 Class A South Embankment Dimensions

The CAS embankment, or cell, is the western fraction of the Federal Cell (Figure 1). The eastern section is occupied by the 11e.(2) cell, which is dedicated to the disposal of uranium processing by-product waste, but not considered in this analysis. A stylized drawing of the CAS and its relationship to the 11e.(2) cell is shown in Figure 2.

The general aspect of the CAS embankment is that of a hipped cap, with relatively steeper sloping sides nearer the edges. The upper part of the embankment, known as the top slope, has a moderate slope, while the side slope is markedly steeper (20% as opposed to 2.4%). These two distinct areas, shown in different colors in Figure 2, are modeled separately in the Clive DU PA model. Each is modeled as a separate one-dimensional column, with an area equivalent to the embankment footprint. The embankment is also constructed such that a portion of it lies below-grade (Figure 2).



**Figure 1. The Clive Facility, with the location of the Class A South embankment outlined in green. This orthophotograph is roughly 1 mile across, and north is up.**

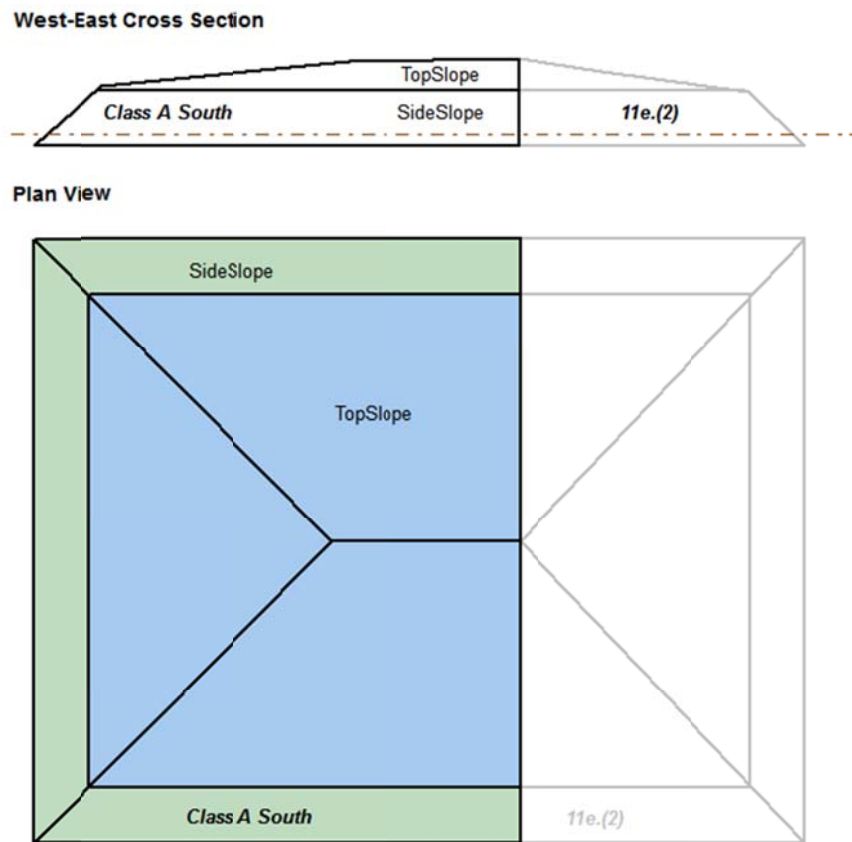


**Figure 2. Section and Plan views of the Class A South embankment, with top slope shown in blue and side slope in green. The brown dotted line in the West-East Cross section represents below-grade (below the line) and above-grade (above the line) regions of the embankment.**

### 3.1.1 Class A South Embankment Interior Waste

The Clive DU PA model requires information about embankment dimensions to be able to determine the footprint areas and the volumes of waste within each area. From this, an average thickness of the waste is determined, since the 1-D column has but one thickness over its entire area. All dimensions provided in this white paper are with respect to the waste itself, and do not include the liner or cover materials. The dimensions of interest that are used in the Clive DU PA model are shown in Figure 3. The values of the dimensions shown in Figure 3 are derived from various engineering drawings in *EnergySolutions* (2009) which are herein referred to in this white paper as drawings 07021 V1, 07021 V3, and 07021 V7. These drawings are all reproduced from *EnergySolutions* (2009) in Figures 4 through Figure 6.

As shown in the engineering drawings, the exact dimensions of the CAS are somewhat irregular, with a gently sloping bottom and ridge line. The shape of the cell has been somewhat idealized to facilitate calculations, and it is assumed to have a horizontal floor and ridge line. Elevations for

the top of the waste are derived from drawing 07021 V1 (Figure 4), which has the note “1. All elevations shown are for top of waste...”. Elevation of the bottom of waste is derived from drawing 07021 V3 (Figure 5). Details on each of these values are provided below.

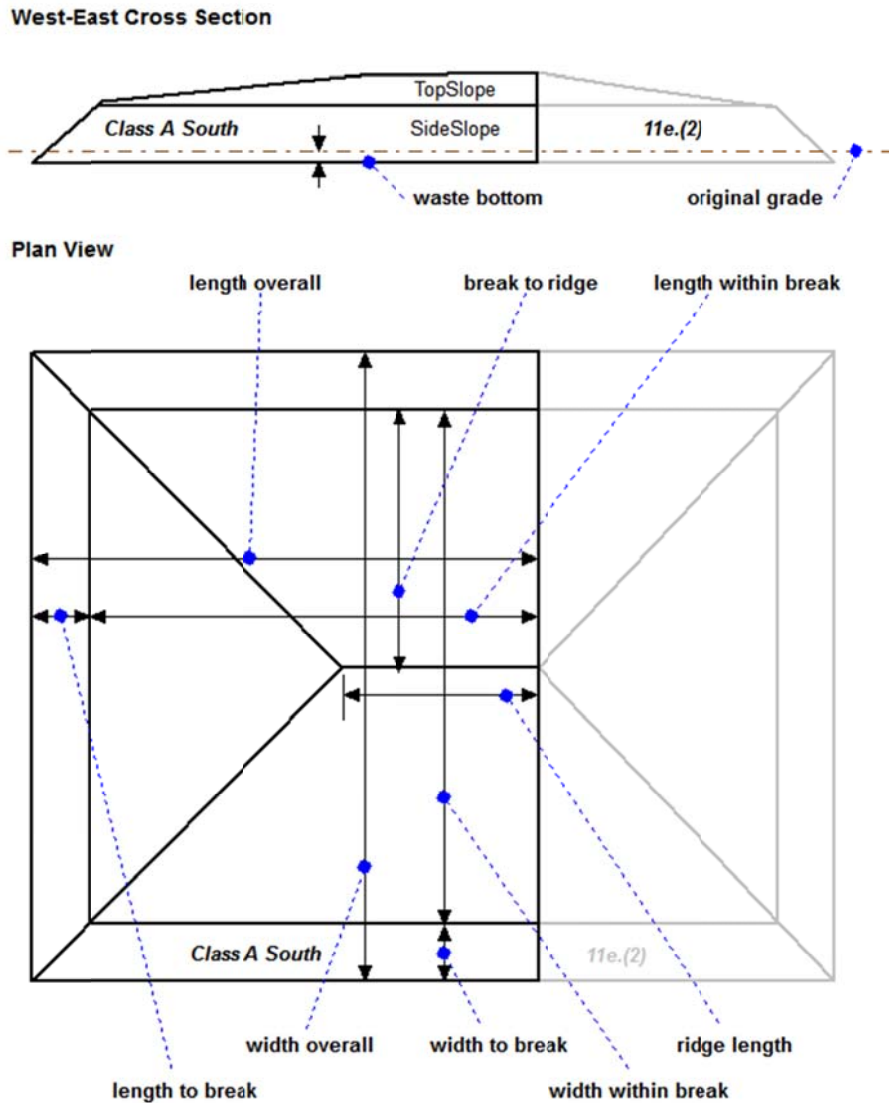


**Figure 3. Dimensions of the Class A South embankment that are used in the Clive DU PA model.**

**Elevation of the top of the waste at the ridge line:** This is calculated as an average of the values from drawing 07021 V3 (Figure 5), West-East Cross Section A, accounting for the 2-ft thick radon barrier. The thickness of the radon barrier, 24 in. (2 ft) is shown in the CAS top slope and CAS side slope sections of drawing 07021 V7 (Figure 6). The top of the radon barrier at the west peak is at 4318.80 ft, so the top of the waste is 2 ft lower at an elevation of 4316.80 ft.

Likewise, the top of the radon barrier at the east peak is 4319.70 ft, so the top of the waste is 2 ft lower at an elevation of 4317.70 ft, after adjusting for the thickness of the radon barrier. The average of the west and east peak elevations is:

$$(4316.80 \text{ ft} + 4317.70 \text{ ft}) / 2 = 4317.25 \text{ ft} \quad (1)$$

**Elevation of the top of the waste at the slope break:** The elevation of the top of the radon barrier derived from the upper drawing 07021 V3 (Figure 5), West-East Cross Section A, is 4301.20 ft. Subtracting the 2-ft thick radon barrier as described above shows the elevation of the top of the waste to be:

$$4301.20 \text{ ft} - 2 \text{ ft} = 4299.20 \text{ ft} \quad (2)$$

**Elevation of the bottom of the waste:** This is calculated as the average of the values derived from the lower drawing 07021 V3 (Figure 5), West-East Cross Section A. The top of the clay liner is at an elevation of 4262.14 ft at the west end, and 4266.19 ft at the east end, which includes the area under the 11e.(2) section of the Federal Cell. The average of these elevations is:

$$(4262.14 \text{ ft} + 4266.19 \text{ ft}) / 2 = 4264.17 \text{ ft} \quad (3)$$

**Length (east-west) overall:** The overall length of the CAS is the sum of the values derived from drawing 07021 V1 (Figure 4). Following along the dimensions shown just below the centerline running west-east, the length is:

$$153.2 \text{ ft} + 734.3 \text{ ft} + 542.1 \text{ ft} = 1429.6 \text{ ft} \quad (4)$$

**Width (north-south) overall:** The overall width of the CAS is the sum of values from drawing 07021 V1 (Figure 4). Following along the dimensions shown down the centerline running north-south, the width is:

$$152.1 \text{ ft} + 735.4 \text{ ft} + 735.4 \text{ ft} + 152.1 \text{ ft} = 1775.0 \text{ ft} \quad (5)$$

**Length from edge to break in slope:** This is derived from drawing 07021 V1 (Figure 4) at the western slope which is 153.2 ft.

**Width from edge to break in slope:** This is derived from drawing 07021 V1 (Figure 4) at the north or south slope which is 152.1 ft.

**Length along the ridge:** The length along the ridge is derived from drawing 07021 V1 (Figure 4) which is 542.1 ft.

### 3.1.2 Class A South Cover and Liner Dimensions

The engineered cover designs for the top slope and side slope sections of the CAS are shown in drawing 07021 V7 (Figure 6). The values chosen from the sections labeled “*Class A South Top Slopes*” and “*Class A South Side Slopes*” are summarized in Table 2. The properties of the various layers within the engineered cover and liner are discussed in detail in *Unsaturated Zone Modeling* white paper.



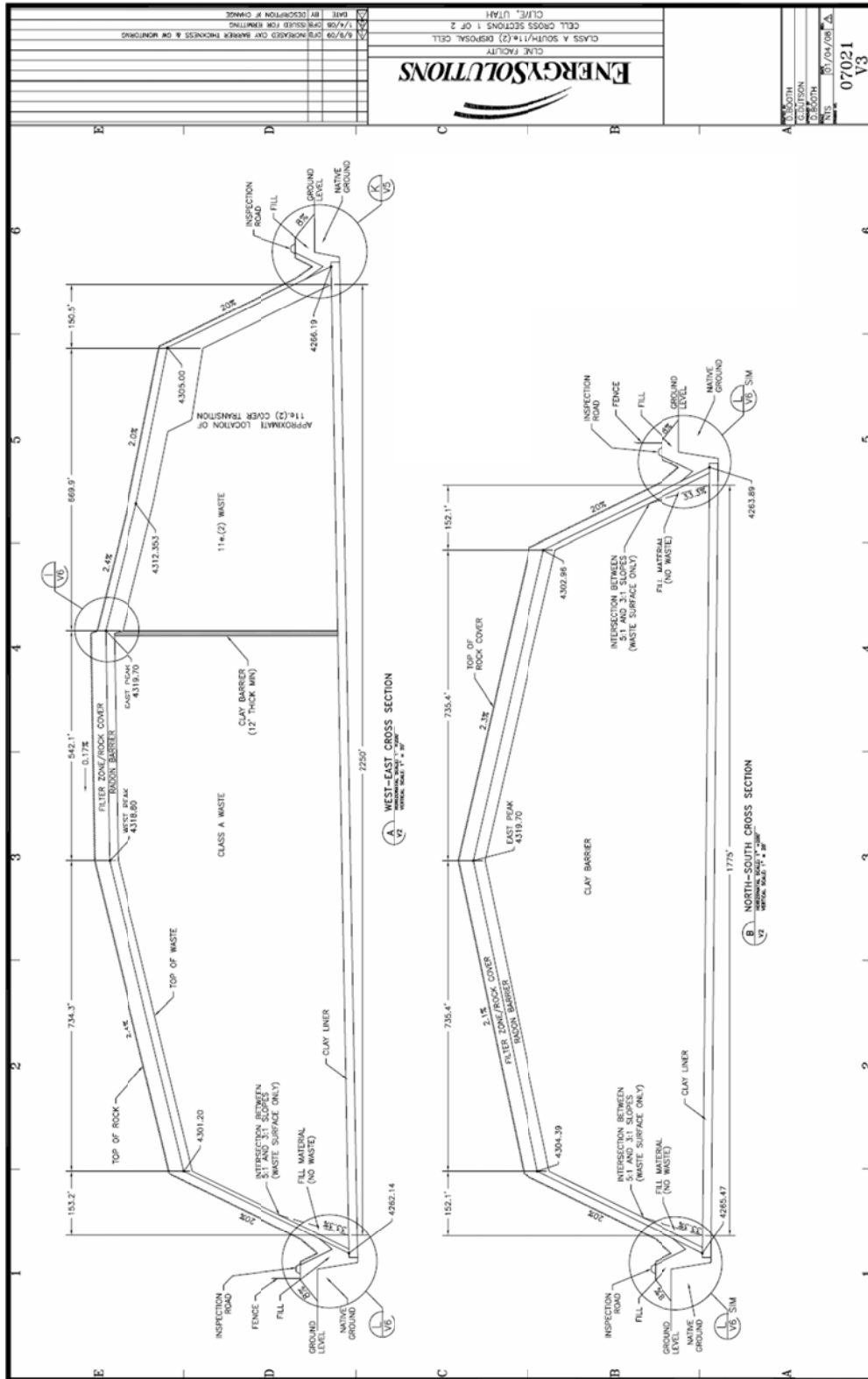


Figure 5. Class A South and 11e.(2) cell engineering drawing 07021 V3

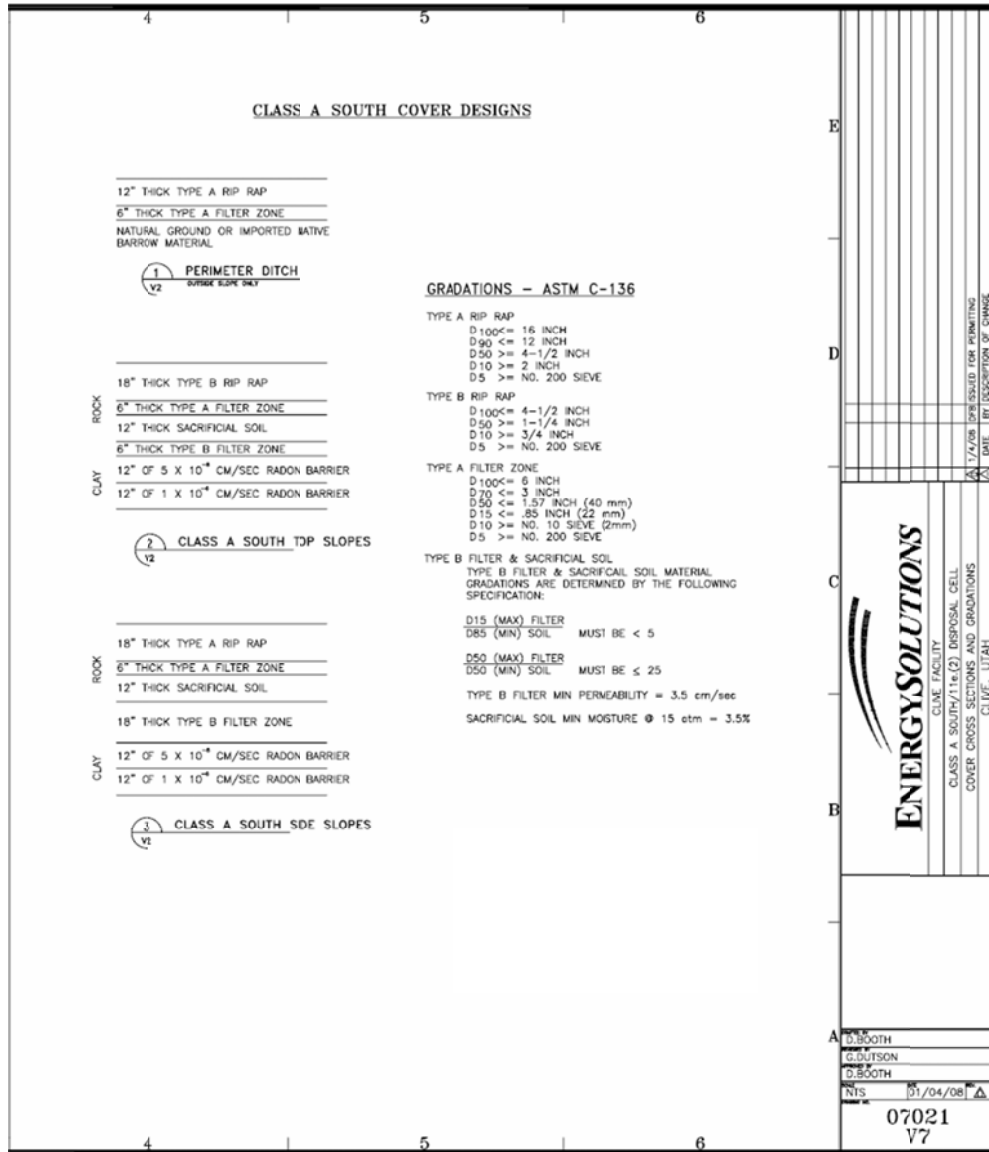


Figure 6. Class A South cell engineering drawing 07021 V7: cap dimensions

**Table 2. Cover layer thicknesses for the CAS cell**

layer	thickness (in)	
	top slope	side slope
type A rip rap	—	18
type B rip rap	18	—
type A filter zone	6	6
sacrificial soil	12	12
type B filter zone	6	18
$5 \times 10^{-8}$ cm/s radon barrier clay	12	12
$1 \times 10^{-6}$ cm/s radon barrier clay	12	12

The waste layers of the embankment are underlain by a clay liner, as shown in Figure 5, but no thickness is provided in this engineering drawing set. The thickness of the clay liner is defined in a previous modeling report as 24 in (2 ft) (Table 7 in Whetstone, 2000).

**Elevation of the bottom of the clay liner:** This is calculated simply the average elevation of the bottom of the waste in eq. (3) minus the thickness of the liner. The elevation of the bottom of the clay liner is then is:

$$4264.17 \text{ ft} - 2 \text{ ft} = 4262.17 \text{ ft} \quad (6)$$

Note that this is also the elevation of the top of the unsaturated zone.

## 4.0 Original Grade Elevation

The original grade is of interest in determining the vertical location of wastes inside the embankment. One might consider any above-ground waste or other material to be erodible, and conversely below-ground portions to be inherently not erodible. It is therefore of interest to determine the disposal volume that lies below grade since placing waste below grade greatly reduces the potential for erosion during lake cycles. Again, only the CAS is considered at this time.

### 4.1 Class A South Embankment Original Grade

The elevation of the original grade is interpreted from the elevations indicated on a 1:24,000 scale quadrangle map for Aragonite, UT (USGS, 1973). The relevant section of this map as it applies to the CAS embankment is shown in Figure 7. This 1-square mile section, Section 32, is the site of the Clive Facility (Figure 7). The southwest corner of Section 32 is at elevation 4270 ft amsl (above mean sea level) while the ground surface (original grade) slopes gently and fairly uniformly up to the northeastern corner, crossing the 4280-ft amsl contour.

The CAS occupies the southwestern corner of Section 32 (refer to Figure 1), and its center is approximately at an elevation of 4272 ft amsl. This is the value used for original grade of the CAS.

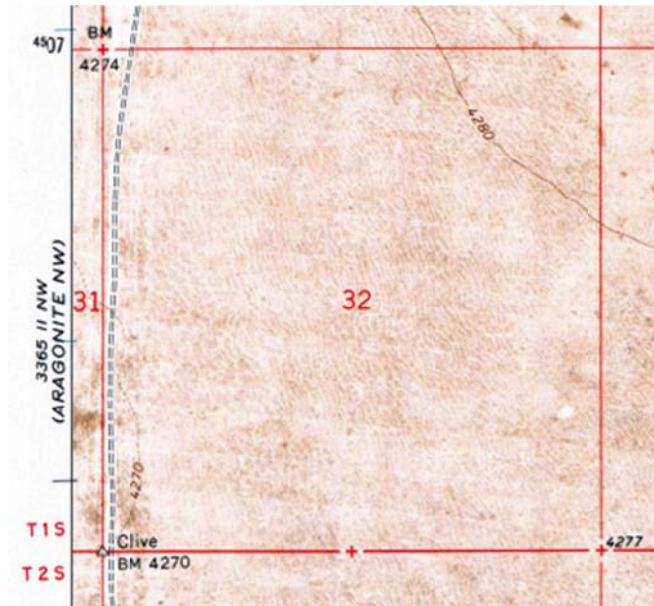


**Figure 7. Section 32 within the Aragonite quadrangle, as it appeared in 1973, before construction of the Clive Facility. Note elevation contours at 4270 and 4280 ft amsl. ARAGONITE NW is the next quadrangle to the west.**

## 5.0 Implementation in the GoldSim Model

### 5.1 Representation of the CAS Embankment

The representation of the CAS embankment in the Clive DU PA Model is essentially one-dimensional (1-D), and is therefore necessarily simplified. The top slope and side slope sections of the embankment are modeled as independent 1-D columns, as discussed below. The volumes of waste and each layer of engineered cap and liner are preserved. Since the cap and liner are laterally continuous and do not vary in dimension within a column, the thicknesses in the model correspond directly to thicknesses in the real world. The waste layers, however, are of a shape that changes in the horizontal, and must be rearranged to produce a shape that is a rectangular prism of equal volume to the actual waste volume.

### 5.1.1 CAS Embankment Dimensions

The dimensions developed in Section 3.1.1 are documented in the model in the container \Disposal\ClassASouthCell\ClassASouth\_Cell\_Dimensions. The calculation of the waste volumes within the side slope and within the top slope, as identified in Figure 2, is done within the GoldSim model by assembling pieces that have volumes that are easily calculated using basic geometry, as shown in Figure 8. Once the waste volumes for top and side slope are known, the average waste thicknesses are calculated. These are used as the waste thicknesses in the columns within the GoldSim model, as described in the following section.

#### Volume Calculations

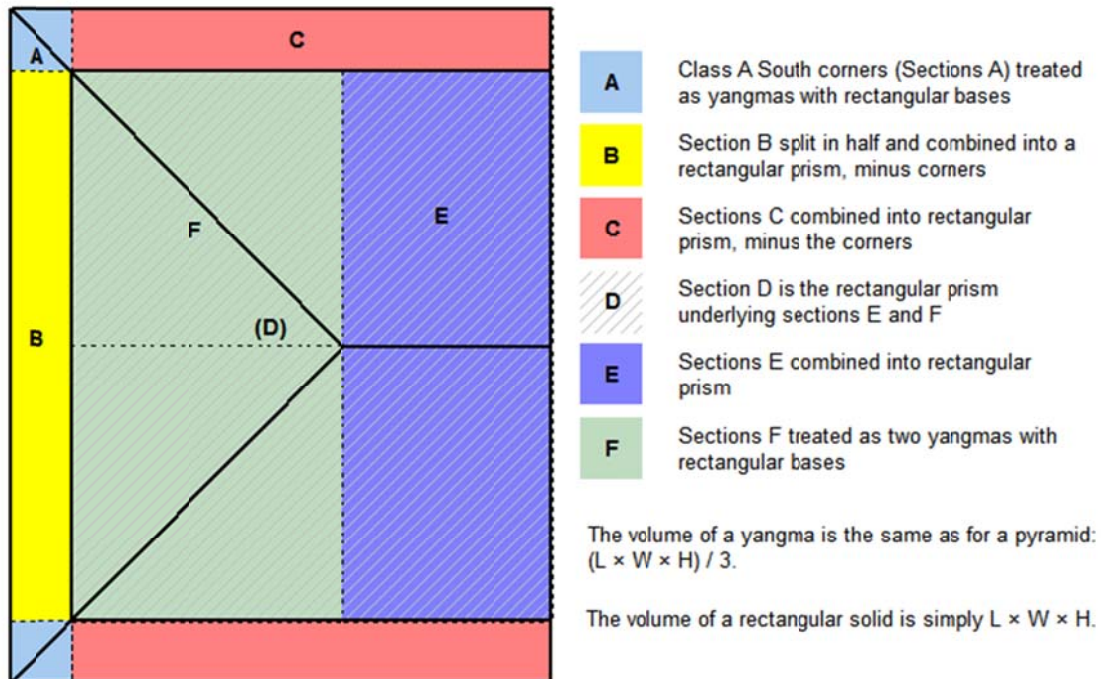


**Figure 8. Geometrical deconstruction of the CAS cell waste volumes**

### 5.1.2 CAS Columns

The top slope and side slope columns are modeled in parallel, since they have different waste and cap layer thicknesses. That is, each column has primarily vertical flow of water, with some lateral flows in the cover. Both feed into the unsaturated zone and thence to groundwater at the bottom. The top slope column has a much thicker waste layer than the side slope, and this is reflected in the overall thickness of the two columns. In order to capture the flexibility available in locating waste during disposal operations, the user can select which waste types go where in the top slope column, using the Waste Layering Definition dashboard. No DU wastes are to be disposed in the side slope column in this model. An example of this selection is shown in Figure 9.

### Definition of Waste Layering for the Class A South Embankment

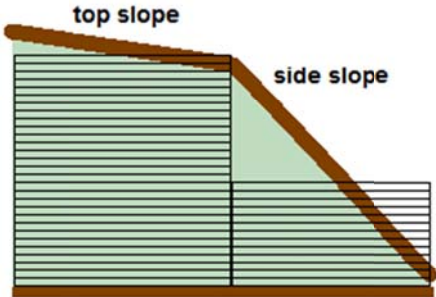
The embankment consists of top slope and side slope sections, each of which is represented by a column of cells with a total thickness equal to the average thickness of the respective column. Each column is broken down into cells of like thickness (within the column), roughly 0.5 m. Each cell may

**Top Slope column**

Top Slope Waste Cell Contents	
Waste01	no waste (clean soil)
Waste02	no waste (clean soil)
Waste03	no waste (clean soil)
Waste04	no waste (clean soil)
Waste05	no waste (clean soil)
Waste06	no waste (clean soil)
Waste07	DUOx: GDP (contaminated)
Waste08	DUOx: GDP (contaminated)
Waste09	DUOx: GDP (contaminated)
Waste10	DUOx: GDP (contaminated)
Waste11	DUOx: GDP (contaminated)
Waste12	DUO3: SRS (contaminated)
Waste13	DUOx: GDP (clean uranium)
Waste14	DUOx: GDP (clean uranium)
Waste15	DUOx: GDP (clean uranium)
Waste16	DUOx: GDP (clean uranium)
Waste17	DUOx: GDP (clean uranium)
Waste18	DUOx: GDP (clean uranium)
Waste19	DUOx: GDP (clean uranium)
Waste20	DUOx: GDP (clean uranium)
Waste21	DUOx: GDP (clean uranium)
Waste22	DUOx: GDP (clean uranium)
Waste23	DUOx: GDP (clean uranium)
Waste24	DUOx: GDP (clean uranium)
Waste25	DUOx: GDP (clean uranium)
Waste26	DUOx: GDP (clean uranium)
WasteOut	DUOx: GDP (clean uranium)

	thickness	volume
each waste cell	0.504 m	8.79e4 m3
entire waste layer	13.61 m	2.373e6 m3

[Exit to Top Slope Wastes](#)



**Side Slope column (currently disabled)**

No DU wastes are allowed in the side slope in this model.

	thickness	volume
each waste cell	0.483 m	2.961e4 m3
entire waste layer	5.792 m	3.553e5 m3

[Exit to Side Slope Wastes](#)

**Summary information**

	Top slope volume	Side slope volume	CAS total volume	bare waste volume	packing efficiency (should be <= 1)
no waste	5.274e5 m3	3.553e5 m3	8.827e5 m3		
Class A Low-Level Waste	0 m3	0 m3	0 m3		
DUO3: SRS (contaminated)	8.79e4 m3	0 m3	8.79e4 m3	2182 m3	0.0248
DUOx: GDP (contaminated)	4.395e5 m3	0 m3	4.395e5 m3	8.833e4 m3	0.201
DUOx: GDP (clean uranium)	1.318e6 m3	0 m3	1.318e6 m3	2.559e5 m3	0.194

*A red X indicates that an inventory volume problem requires resolution.*

[Go to Material Properties](#)
[CAS Inventory Definitions](#)
[Exit to Class A South](#)
[Control Panel](#)

Figure 9. Waste layering definitions within the two columns of the CAS cell

## 6.0 References

EnergySolutions, 2009. *EnergySolutions License Amendment Request: Class A South/11e.(2) Embankment, Revision 1*, 9 June 2009 (file: Class A South-11e.(2) Eng Drawings.pdf)

GTG (GoldSim Technology Group), 2010. *GoldSim: Monte Carlo Simulation Software for Decision and Risk Analysis*, <http://www.goldsim.com>

USGS (United States Geological Survey), 1973. 1:24,000 topographic quadrangle map for Aragonite, UT, revised 1973 (file: UT\_Aragonite\_1973\_geo.pdf)

Whetstone (Whetstone Associates, Inc.), 2000. Revised Envirocare of Utah Western LARW Cell Infiltration and Transport Modeling (file: 2000, July 19 - Whetstone, Western LARW Cell Infiltration Modeling.pdf)

# Implementation of Diffusion in GoldSim

Kate Catlett  
John Tauxe  
Neptune and Co.  
April 2011

## Introduction

This paper outlines how diffusion in air and water is to be implemented in GoldSim models that include diffusion in the unsaturated zone. The need for this discussion arises from the assumption in GoldSim that diffusion occurs only in saturated porous media. In the modeling of radioactive waste facilities, we have the definite need to include diffusion in both the air phase (e.g. diffusion of radon from buried wastes to the ground surface) and often in the water phase. These processes can be independently enabled or disabled by setting logical “switches” in the model.

We have tested diffusion-specific models built in GoldSim for consistency with analytical results, and have verified our interpretation of GoldSim’s internal calculations, and the appropriateness of our modifications to definitions of diffusive flux.

## Diffusion Math

To introduce basic diffusive transport mathematics, we turn to Jury (1991), who provides the following 1-dimensional gas phase conservation (transport) equation:

$$\frac{\partial \theta_a C_g}{\partial t} = - \frac{\partial J}{\partial z} \quad [1]$$

where

$\theta_a$  = volumetric air content (constant in space and time),

$C_g$  = gas concentration in air,

$t$  = time, and

$z$  = the single spatial dimension,

and the diffusive mass flux  $J$  is given by

$$J = -D_g^s \frac{\partial C_g}{\partial z} \quad [2]$$

where the effective diffusion coefficient  $D_g^s$  is

$$D_g^s = \tau_a \cdot D \quad [3]$$

where

$\tau_a$  = tortuosity of the air phase and

$D$  = free air molecular diffusion coefficient (also called the free air diffusivity).

Combining equations [1], [2], and [3], we find that

$$\frac{\partial \theta_a C_g}{\partial t} = \frac{\partial}{\partial z} \left( \tau_a \cdot D \frac{\partial C_g}{\partial z} \right) \quad [4]$$

## Diffusion in GoldSim

In the GoldSim modeling environment, the flux equation looks like (GoldSim CT manual p. B-4, Eq. B-3):

$$J = D_{cs} (C_i - C_j) \quad [5]$$

where

- $J$  = diffusive mass flux,
- $D_{cs}$  = GoldSim's "diffusive conductance",
- $C_i$  = concentration in cell  $i$  in air (essentially  $C_g$ ), and
- $C_j$  = concentration in cell  $j$  in air (essentially  $C_g$ ).

Note that GoldSim uses the concentration difference, not the gradient, in the fluid medium in question. The gradient is the difference divided by the diffusive length (in GoldSim, this is the sum of the diffusive lengths defined in each adjacent cell). Diffusive conductance is defined as (GoldSim CT manual p. B-5, Eq. B-5):

$$D_{cs} = \frac{A_c}{\frac{L_{ci}}{f_{ms} \cdot d_{ms} \cdot t_{Pci} \cdot n_{Pci}} + \frac{L_{cj}}{f_{ns} \cdot d_{ns} \cdot t_{Pcj} \cdot n_{Pcj} \cdot K_{nms}}} \quad [6]$$

where

- $A_c$  = the bulk cross-sectional area of diffusive mass flux link,
- $L_{ci}$  = diffusive length in cell  $i$ ,
- $L_{cj}$  = diffusive length in cell  $j$ ,
- $f_{ms}$  = available porosity for species  $s$  in medium  $m$  (i.e., the fraction of the pore volume of solid  $m$  that is accessible to species  $s$ ),
- $f_{ns}$  = available porosity for species  $s$  in medium  $n$  (i.e., the fraction of the pore volume of solid  $n$  that is accessible to species  $s$ ),
- $d_{ms}$  = diffusivity for species  $s$  for fluid  $m$  (in cell  $i$ ),
- $d_{ns}$  = diffusivity for species  $s$  for fluid  $n$  (in cell  $j$ ),
- $t_{Pci}$  = tortuosity for the porous medium in cell  $i$  ( $t \leq 1$ ),
- $t_{Pcj}$  = tortuosity for the porous medium in cell  $j$  ( $t \leq 1$ ),
- $n_{Pci}$  = porosity for the porous medium in cell  $i$ ,
- $n_{Pcj}$  = porosity for the porous medium in cell  $j$ , and
- $K_{nms}$  = partition coefficient between fluid medium  $n$  (in cell  $j$ ) and fluid medium  $m$  (in cell  $i$ ) for species  $s$ .

This equation can be greatly simplified if we ignore the “available porosity” factors (let the equal 1) and assume no suspended solids, one porous medium (partition coefficients, porosities and tortuosities are the same) and one fluid medium (diffusivities are the same):

$$D_{cs} = \frac{AnD\tau}{L} \quad [7]$$

where

- $A$  = diffusive area, or bulk cross-sectional area of the porous medium,
- $n$  = total porosity of the porous medium,
- $D$  = free air diffusivity (same as  $D$  above),
- $\tau$  = tortuosity of the entire pore space in the porous medium, and
- $L$  = the sum of the diffusive lengths in adjacent cells  $i$  and  $j$ .

It is useful to determine at this point exactly where each of these values comes from in GoldSim. The diffusive area and diffusive lengths are provided explicitly to GoldSim in the definition of each diffusive flux link, using Diffusive Fluxes tab in the Cell Pathway Properties dialog box shown in Figure 1.

## Diffusion in Partially-Saturated Porous Media

This dialog box also provides for the definition of the porous medium, in this example “Alluvium”, which has the properties of porosity and tortuosity as part of its definition as a solid material. It is important to note that the values of porosity and tortuosity used in GoldSim’s calculation of diffusive flux are taken from the definition of the solid material, and *GoldSim assumes that the porous medium is saturated with respect to the fluid through which diffusion is occurring*. This assumption is violated for unsaturated conditions. In the current example, we wish to allow diffusion in both Water and Air fluids, so some corrections have to be applied to the values for porosity  $n$  and tortuosity  $\tau$ . Instead of using the Alluvium’s defined  $n$  and  $\tau$ , we need to use values appropriate for the fluid of interest. For example, for air, we want to use volumetric air content  $\theta_a$  instead of  $n$ , and air-phase tortuosity  $\tau_a$  instead of a generalized  $\tau$ . Since GoldSim is hard-coded to apply the  $n$  and  $\tau$  for the solid material (Alluvium), we need to account for the differences carefully.

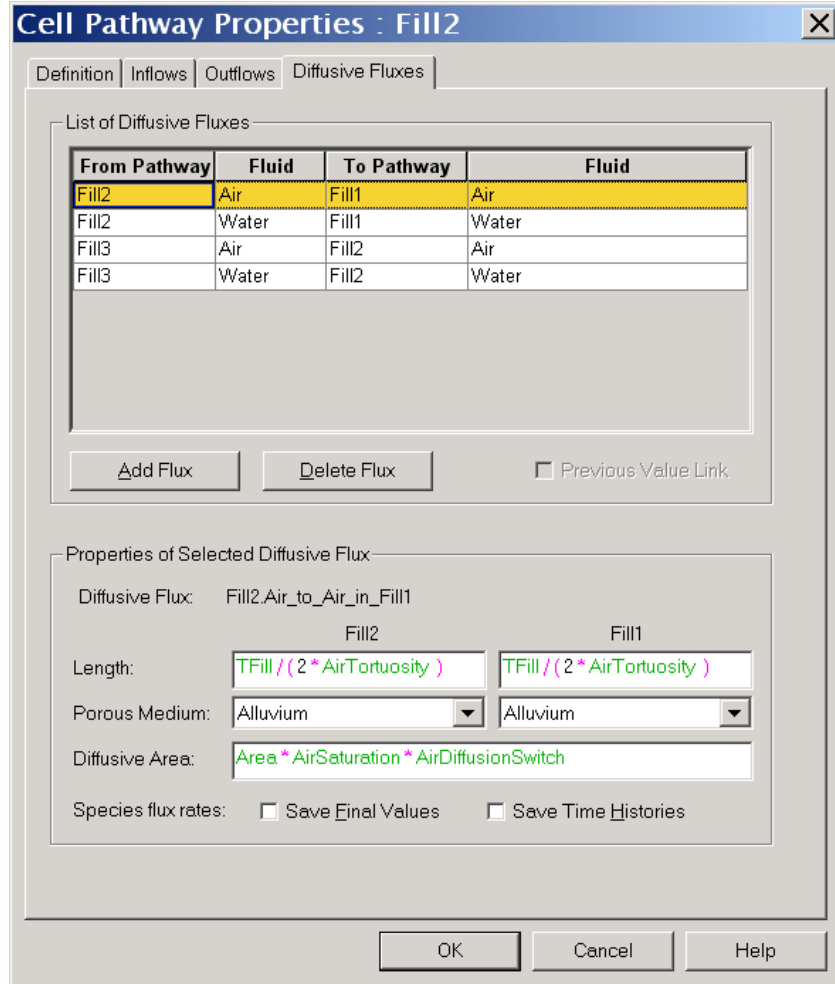


**Figure 1. The definition of diffusive flux in GoldSim**

In order to use volumetric air content instead of porosity, we insert a multiplicative factor into the definition of the Diffusive Area, so that we get the cross-sectional area of the fluid of interest, rather than the entire porous medium (see Figure 1). GoldSim internally multiplies the Diffusive Area times the Alluvium porosity  $n$ , so we must multiply that by the Air phase saturation,  $S_a$ , to get

$$D_{cs} = \frac{AS_a n D \tau}{L} \quad [8]$$

so that GoldSim ends up working with the cross-sectional area of just the Air phase, which is  $A\theta_a$ :

$$D_{cs} = \frac{A\theta_a D \tau}{L} \quad [9]$$

An alternative approach would be to define the porosity of the Alluvium to be unity, and correct the Diffusive Area by  $\theta_a$  rather than by  $S_a$ . This approach, however, has

unintended consequences since other processes (such as retardation) use the porosity value defined for Alluvium.

In addition to the area correction to account for partially-saturated media, we need to use an appropriate value for tortuosity. What we want is the tortuosity of the phase in which diffusion occurs, but again, GoldSim assumes saturation and is hard-coded to use the bulk tortuosity defined for the porous medium, Alluvium. In this case, it is simplest to effectively remove the porous medium tortuosity by setting it equal to 1 in the definition of the Alluvium, and to apply fluid-specific tortuosities in the definition of the Diffusive Flux. The logical parameter to modify is the Diffusive Length, since the concept of porosity is one of increased distance of travel that a diffusive species must travel due to its tortuous path through the partially-saturated porous medium. Fortunately, no other processes in GoldSim use the tortuosity value specified for Alluvium, so defining it as unity does not affect other parts of the model.

We have adopted the definition of tortuosity as the straight-line path between points A and B in the porous medium divided by the actual path through the fluid, tortuosity values are always between 0 and 1, with lower values implying more tortuous paths. The corrected Diffusive Length, therefore, is  $L / \tau_a$  (for Air in this case). This correction can be seen in Figure 1. In effect, GoldSim is then solving the equation (for Air)

$$D_{cs} = \frac{A\theta_a D \tau_a}{L} \quad [9]$$

For the water phase, the analogous equation is found by substituting  $\theta_w$  and  $\tau_w$  for  $\theta_a$  and  $\tau_a$ . While values for  $\theta_w$  and  $\theta_a$  are simple in concept and derivation, the fluid-specific tortuosities are not. Their derivation is the subject of a discussion below.

## Grappling with Tortuosity

Jury (1991) discusses models for estimating air-phase tortuosity from other material properties, such as water content and porosity. In Jury's Table 6.1, the following three models are presented:

**Table 1. Air phase tortuosity equations.**

equation for air phase tortuosity	reference
$\tau_a = \frac{\theta_a^{10/3}}{n^2}$	Millington and Quirk (1961)
$\tau_a = 0.66\theta_a$	Penman (1940)
$\tau_a = \theta_a^{3/2}$	Marshall (1959)

At air contents and porosities typical of arid sites, however, these models give markedly different results. If we assume a porosity of 0.39 and a water content of 0.06, then we have an air content of 0.30. The three models return values for air phase tortuosity of 0.12, 0.88, and 0.16, respectively, showing wide variation in their estimates. Which model is most appropriate for a given material is a matter of site-specific investigation.

Also undetermined is an appropriate model for water phase tortuosity.

## Modeling with GoldSim vs FEHM

The solution to GoldSim's unsaturated diffusive flux problem was originally developed while modeling the Radioactive Waste Management Sites (RWMSs) at the Nevada National Security Site (NNSS, formerly the Nevada Test Site). Since the issues surrounding the migration of water in the unsaturated zone at the NNSS were addressed by practitioners at Los Alamos National Laboratory (LANL) using the FEHM modeling program, we examined the implementations of diffusive flux in GoldSim and in a FEHM-based unsaturated zone model developed by Walvoord, Wolfsberg and Stauffer. This is important for consistency between the GoldSim and FEHM models of the unsaturated zone at the RWMSs.

Returning to the simplified version of GoldSim's equation for Diffusive Flux modified for a single fluid phase (equation [9]), we can substitute that equation into the mass balance equation (GoldSim CT manual p. B-2, Eq. B-1), giving

$$\frac{\partial m}{\partial t} = \frac{A}{L} \theta_a \tau_a \cdot D (C_i - C_j) \quad [10]$$

We can convert mass to concentration (in air, rather than bulk concentration) since  $m = C_g \theta_a V$ , and rearrange to look more like the equation from Jury (Eq. 4)

$$\frac{\partial \theta_a C_g}{\partial t} = \frac{A}{V L} [\theta_a \tau_a \cdot D (C_i - C_j)] \quad [11]$$

where  $V$  is the volume of the cell. Dividing through by  $\theta_a$  gives

$$\frac{\partial C_g}{\partial t} = \frac{A}{V L} [\tau_a \cdot D (C_i - C_j)] \quad [12]$$

The key is seeing that the definition of  $D_g^s$  in the Jury text does not explicitly include volumetric air content. From Eq. 11, we can see that GoldSim *does* explicitly include volumetric air content (or rather, porosity) in the definition of  $D_g^s$  (or  $D_{cs}$ ), so that  $D_g^s$  is defined as

$$D_g^s = \theta_a D \tau_a$$

Note that FEHM, like GoldSim, includes volumetric air content explicitly.

Thus we must be careful when we define the air phase tortuosity  $\tau_a$  in our model in order to understand how  $D_g^s$  is defined in the literature that the various tortuosity equations come from. For example, Jury (1991) writes the Millington-Quirk (1961) equation for air phase tortuosity as  $\frac{\theta_a^{10/3}}{n^2}$  (where  $n$  is porosity) and in GoldSim we need to use  $\frac{\theta_a^{7/3}}{n^2}$  for tortuosity.

## References

Jury, W.A., W.R. Gardner, and W.H. Gardner, 1991. *Soil Physics* Fifth Edition, Wiley, New York, NY

Marshall, T.J., 1959. "The diffusion of gas through porous media." *Journal of Soil Science* (10) pp. 79-82

Millington, R.J., and J.P. Quirk, 1961. "Permeability of porous solids." *Trans. Faraday Society* (57) pp. 1200-1207

Penman ----1940 -----(referenced in Jury 1991)

# Ionic Diffusion Coefficients for Transport Modeling in GoldSim

Dave Gratson  
Neptune and Company  
February 2010

Recent discussions about the diffusion coefficients currently used in contaminant transport models in GoldSim have centered on exploring ion-specific  $D_m$  values, as opposed to the single value of  $4.3 \times 10^{-5} \text{ cm}^2/\text{s}$  for transuranics (TRU) as used in the Performance Assessment (PA) for the Greater Confinement Disposal (GCD) boreholes at the NTS (Cochran, et al. 2001). The GCD PA justifies the use of this value thus: “The molecular diffusion coefficient is not radionuclide -specific ... because the radionuclides themselves are of similar size.” While that may hold true for the TRU waste in the GCD boreholes, it most definitely is not true for the wide variety of radionuclides found in low-level radioactive wastes disposed in other facilities.

I investigated approaches for incorporating individual  $D_m$  values for the chemical elements in the model, a long list spanning most of the periodic table with extreme ranges of ion sizes. Thus it would seem prudent to derive  $D_m$  values for each element used in the model. However, after investigating this issue I will provide two arguments for using a range of  $D_m$  values, rather than attempting to provide individual values.

$D_m$  derivation: Ionic and molecular diffusion coefficients are derived in theory from the Stokes-Einstein equation:

$$D_{AB} = RT/6\pi \eta_B r_A,$$

where

- R = universal gas constant,
- T = temperature,
- $\eta_B$  = absolute viscosity of the solvent (water), and
- $r_A$  = radius of the “spherical” solute.

A variety of empirical equations have been derived based on the Stokes-Einstein equation for different scenarios. For a dilute solution of a single salt the diffusion coefficient can be derived from the Nernst-Haskell equation (Reid et al., 1987). This equation includes the valence of the cation and anions as well as ionic conductances. Specific ionic conductances are required for each cation and anion species. When two or more chemical species are present at different concentrations, interdiffusion (counterdiffusion) must be included to satisfy electroneutrality (Lerman 1979). For a geochemical system as large as that found in LW disposal facilities this quickly becomes too complex to model, even if ionic conductivities are available for each species.

The second difficulty in deriving diffusion coefficients lies in the large number of potential ions. The number of LLW elements typically modeled may be 30 to 40, and for each element in this list one can expect multiple forms. For example, U has 4 redox states, and many soluble species for each of these. Assuming oxic conditions U will be primarily found as  $\text{UO}_2(\text{CO}_3)_3^{-4}$ ,  $\text{UO}_2(\text{CO}_3)_2^{-2}$ , and  $\text{UO}_2\text{CO}_3^0$ , however there are at least 8

additional forms of U(+6) that may be found. Thus the potential number of ions that would need to be included in the model would easily be in the hundreds. Obtaining the parameters for each species that would be required to model the ionic diffusion would be difficult.

Solution: I propose a  $D_m$  range be incorporated. This range can be derived from Table 3.1 in Lerman (1979). For conditions near 25°C, the range of  $D_m$  for the elements of interest is  $4 \times 10^{-6}$  to  $2 \times 10^{-5}$  cm<sup>2</sup>/s. For cooler temperatures, which would be expected in the deeper subsurface, the values are somewhat lower. The values for 25°C are reproduced in the following table:

Cation	$D_m$ (10 <sup>-6</sup> cm <sup>2</sup> /s)	Anion	$D_m$ (10 <sup>-6</sup> cm <sup>2</sup> /s)
K <sup>+</sup>	19.6	Cl <sup>-</sup>	20.3
Cs <sup>+</sup>	20.7	I <sup>-</sup>	20.0
Sr <sup>2+</sup>	7.94	IO <sub>3</sub> <sup>-</sup>	10.6
Ba <sup>2+</sup>	8.48		
Ra <sup>2+</sup>	8.89		
Co <sup>2+</sup>	6.99		
Ni <sup>2+</sup>	6.79		
Cd <sup>2+</sup>	7.17		
Pb <sup>2+</sup>	9.45		
UO <sub>2</sub> <sup>2+</sup>	4.26		
Al <sup>3+</sup>	5.59		

from Table 3.1 in Lerman (1979)

Based on this discussion, the value chosen for the GoldSim element \Materials\Water\_Properties\Dm is a uniform stochastic, varying from  $3 \times 10^{-6}$  to  $2 \times 10^{-5}$  cm<sup>2</sup>/s.

## References

- Cochran, J.R., W.E. Beyeler, D.A. Brosseau, L.H. Brush, T.J. Brown, B.M. Crowe, S.H. Conrad, P.A. Davis, T. Ehrhorn, T. Feeney, W. Fogleman, D.P. Gallegos, R. Haaker, E. Kalinina, L.L. Price, D.P. Thomas, and S. Wirth, 2001. *Compliance Assessment Document for the Transuranic Wastes in the Greater Confinement Disposal Boreholes at the Nevada Test Site, Volume 2: Performance Assessment*, SAND2001-2977, September 2001
- Lerman, A. 1979. *Geochemical Processes in Water and Sediment Environments*. Wiley-Interscience. QES71.L45
- Reid, Prausnitz, and Poling, 1987. *The Properties of Gases and Liquids*, 4<sup>th</sup> Edition. McGraw-Hill, Inc. TP242.R4